Available online at www.sciencedirect.com
SCIENCE DIRECT®
C. R. Physique 6 (2005) 1059–1069
COMPTES RENDUS PHYSIQUE
http://france.elsevier.com/direct/COMREN/

MCAO for very large telescopes/OAMC pour les très grands télescopes

Optimal control for Multi-Conjugate Adaptive Optics

Cyril Petit [a], Jean-Marc Conan [a,*], Caroline Kulcsár [b], Henri-François Raynaud [b], Thierry Fusco [a], Joseph Montri [a], Didier Rabaud [c]

[a] *Office national d'études et de recherches aérospatiales, BP 72, 92322 Châtillon cedex, France*
[b] *Université Paris 13, institut Galilée, L2TI, 93430 Villetaneuse, France*
[c] *Shaktiware, 27, boulevard C. Moretti, 13014 Marseille, France*

Abstract

Classic adaptive optics (AO) is now a proven technique that provides a closed loop real time correction of the turbulence. It is generally based on simple and efficient control algorithms. The next AO generation (Multi-Conjugate AO (MCAO) in its various forms and Extreme AO (XAO)) will require more sophisticated control approaches, especially in the case of wide field AO. We present here the concepts behind optimal control. The advantages compared to more standard approaches are stressed. A first experimental validation is presented. ***To cite this article: C. Petit et al., C. R. Physique 6 (2005).***

Résumé

Contrôle optimal pour l'optique adaptative multi-conjuguée. L'Optique Adaptative (OA) classique est aujourd'hui une technique éprouvée permettant une correction temps réel en boucle fermée des effets de la turbulence. Généralement, elle se base sur des lois de commande simples et efficaces. Cependant, les futures générations d'OA (Optique Adaptative Multi-conjuguée (OAMC) dans ces diverses formes et l'OA Extreme), nécessiteront des lois de contrôle plus sophistiquées en particulier dans le cas de l'OA grand champ. Nous présentons dans cet article une solution de contrôle optimal pour l'OA en général, et mettons en évidence ses atouts comparativement aux approches standard. Une première validation expérimentale de cette approche est présentée. ***Pour citer cet article : C. Petit et al., C. R. Physique 6 (2005).***

Keywords: Adaptive optics; Kalman filter; Control theory

Mots-clés : Optique adaptative ; Filtre de Kalman ; Automatique

1. Introduction

Classic Adaptive Optics [AO] [1] and Multi-Conjugate AO [MCAO] [2–4] have similarities in terms of formalism and system structure. In both cases we have a real time closed loop system with delay and, in a first approximation, a linear model for the Wave Front Sensor (WFS) measurements and for the Deformable Mirror (DM) correction. We show how to derive an

* Corresponding author.
E-mail addresses: cpetit@onera.fr (C. Petit), conan@onera.fr (J.-M. Conan), kulcsar@l2ti.univ-paris13.fr (C. Kulcsár), Henri-Francois.Raynaud@l2ti.univ-paris13.fr (H.-F. Raynaud), fusco@onera.fr (T. Fusco), montri@onera.fr (J. Montri), didier.rabaud@shaktiware.fr (D. Rabaud).

1631-0705/$ – see front matter
doi:10.1016/j.crhy.2005.10.013

optimal control in this context. The problem actually breaks down into a stochastic estimation of the turbulent phase, followed by a deterministic control problem. With the usual assumptions made in AO/MCAO, the estimation problem can be solved by Kalman filtering [5,6].

MCAO still has some specificities: it deals with a large number of degrees of freedom, the WFS measurements are available only in particular directions corresponding to the Guide Stars (GSs). Achieving a good correction in a large Field of View (FoV) implicitly requires to interpolate the WFS measurements between the GSs. It implies a careful reconstruction process using prior information on the turbulent volume [7]. This leads to a global optimization of the multi-variable servo-loop [6,8]. The extension to MCAO [9] of more standard techniques providing a mode per mode optimization [10–13] is also discussed.

The gain in performance brought by optimal control is illustrated in the particular case of tomographic Off-Axis Adaptive Optics [OAAO] [14,15]. A first experimental demonstration is presented in this context.

We first present the principle of optimal control for AO/MCAO in Section 2. A step by step construction of the optimal closed-loop control is proposed by defining different formal sub-problems (see Section 2.1). The sub-problems that have to be solved are the following: WFS reconstruction (see Section 2.2), correction in open-loop (see Section 2.3), correction in closed-loop (see Section 2.4). For each case we define an optimal solution based on an explicit optimality criterion. We also consider more straightforward solutions and discuss the underlying implicit prior models. For the sake of simplicity the formalism is first given for classic AO, and then generalized to MCAO in Section 2.5 where the specificities of such systems are discussed. Finally, an experimental validation of optimal control is given in Section 3 in the particularly illustrative case of tomographic OAAO. The principle of OAAO is recalled (see Section 3.1) and experimental results are shown and compared to the expected performance obtained by simulation (see Section 3.2).

2. Optimal control formalism

We will address in this section three different formal sub-problems that are summarized in Fig. 1: wave-front reconstruction, open-loop and closed-loop correction. Wave-front reconstruction is an estimation problem which consists in evaluating the turbulent phase from WFS measurements. The open/closed-loop corrections are control issues which consist in determining the DM voltages from WFS measurements. In the open-loop case the WFS directly sees turbulent wave-fronts, the DM being located down-stream. In the closed-loop case the DM is up-stream and the WFS sees residual wave-fronts after correction.

These three topics will be shown to be strongly related. For each scenario an explicit optimality criterion will be defined and the optimal solution will be derived. The potential advantages of the optimal approach, compared to more straight-forward methods, will be stressed.

2.1. Problem formulation

The turbulent phase integrated over the time interval $[(n-1)T, nT]$ will be denoted ϕ_n. T is the sampling period corresponding to the WFS exposure time. With such a discretization the problems addressed here can be treated with discrete quantities without any loss of generality [16]. The turbulent phase is described here by its Zernike polynomial expansion. ϕ_n is therefore a vector of Zernike coefficients.

In all three scenarios a description of the WFS measurements is needed. Considering a linear model, the WFS measurement that becomes available in the time interval $[(n-1)T, nT]$ is given by:

$$\mathbf{s}_n = \mathbf{D}\phi^{\text{wfs}}_{n-dr} + \mathbf{w}_n \tag{1}$$

where $\mathbf{D}$ is a matrix characterizing the WFS, ϕ^{wfs}_{n-dr} is the phase seen by the WFS, and $\mathbf{w}_n$ is the measurement noise. The parameter dr denotes the 'read-out' delay. It accounts for the fact that the measurement related to the phase in a given time interval is generally not instantaneously available due to signal read-out and processing time.

Note that in open-loop the WFS phase ϕ^{wfs}_n is the turbulent phase, ϕ_n, while in closed-loop it is the residual phase after correction, $\phi_n - \phi^{\text{cor}}_n$.

The first question addressed here is the optimal phase reconstruction from noisy open-loop WFS measurements. The objective is then to estimate, and even predict, the turbulent phase at a given time step. Let us assume that we are interested in ϕ_{n+1}. Its optimal estimate $\hat{\phi}_{n+1}$ is defined by minimizing, over turbulence and WFS noise statistics, the estimation error variance:

$$\epsilon_{\text{est}} = \left\langle \|\phi_{n+1} - \hat{\phi}_{n+1}\|^2 \right\rangle_{\text{turb,noise}} \tag{2}$$

The estimate $\hat{\phi}_{n+1}$ has to be deduced from the past available WFS data $\{\mathbf{s}_n, \mathbf{s}_{n-1}, \mathbf{s}_{n-2}, \ldots\}$. Section 2.2 solves this problem in the case of open-loop measurements. The generalization to closed-loop data is given in Section 2.4.

In any case, the optimal reconstruction requires statistical priors on turbulent phase and WFS noise. We assume a temporally white noise with centered Gaussian statistics of covariance matrix $\mathbf{C}_w$. The phase will be supposed to follow centered Gaussian

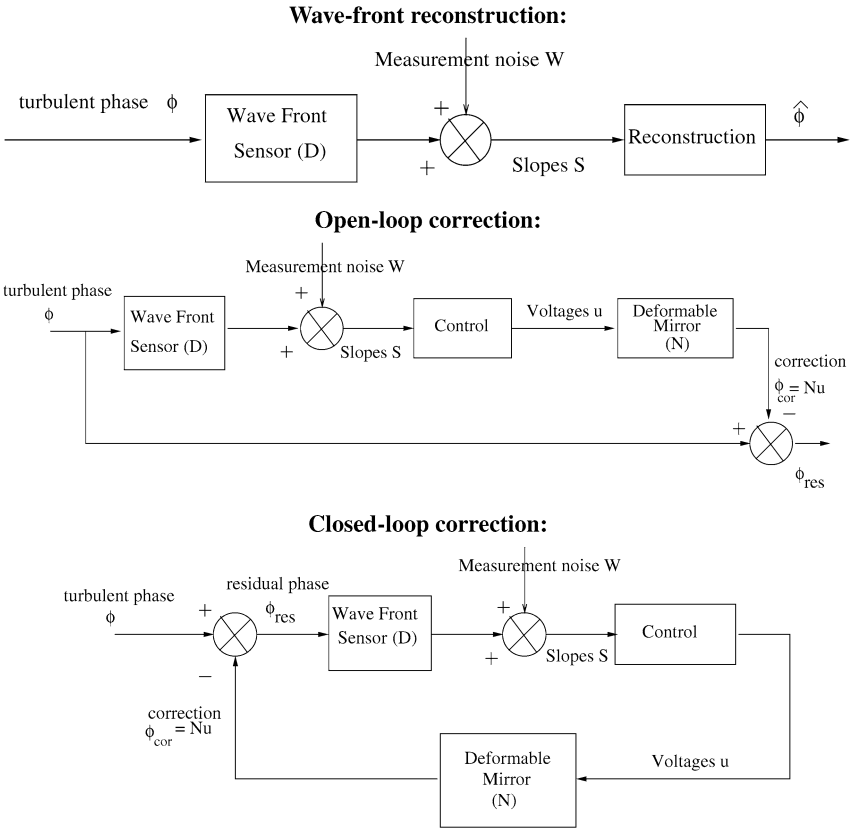

Fig. 1. Block-diagrams corresponding to the three sub-problems addressed here: wave-front reconstruction, open-loop and closed-loop correction.

statistics with a known covariance matrix $\mathbf{C}_\phi$ [17]. Different temporal models [5,18,19,6] can be constructed to account for the evolution in time of the turbulent phases. Here we will use a first order auto-regressive model in the form:

$$\phi_{n+1} = \mathbf{A}_{\text{tur}}\phi_n + \nu_n \tag{3}$$

where ν_n is a white noise of covariance matrix $\mathbf{C}_\nu$. The matrix $\mathbf{A}_{\text{tur}}$ defines the temporal correlation of each Zernike component of the phase. Ensuring the conservation of the global energy of the turbulence then leads to:

$$\mathbf{C}_\nu = \mathbf{C}_\phi - \mathbf{A}_{\text{tur}}^t \mathbf{C}_\phi \mathbf{A}_{\text{tur}} \tag{4}$$

Regarding correction, if any, the correction phase ϕ_{n+1}^{cor} is produced by the last calculated DM voltages $\mathbf{u}_n$ which are kept constant during the time interval $[nT, (n+1)T]$. Assuming for the DM a linear behavior with instantaneous time response, we can write:

$$\phi_{n+1}^{\text{cor}} = \mathbf{N}\mathbf{u}_n \tag{5}$$

where $\mathbf{N}$ is the influence matrix.

The control voltages $\mathbf{u}_n$ are estimated from the WFS data available in the time interval $[(n-1)T, nT]$, that is $\{\mathbf{s}_n, \mathbf{s}_{n-1}, \mathbf{s}_{n-2}, \ldots\}$.

The optimization problem consists here in finding the correction voltages that minimize the residual phase variance, hence minimizing the following criterion:

$$\epsilon_{\text{cor}} = \left\langle \left\| \phi_{n+1} - \phi_{n+1}^{\text{cor}} \right\|^2 \right\rangle_{\text{turb,noise}} = \left\langle \left\| \phi_{n+1} - \mathbf{N}\mathbf{u}_n \right\|^2 \right\rangle_{\text{turb,noise}} \tag{6}$$

The separation principle [20] tells us that this is equivalent to solve the stochastic reconstruction problem presented before, minimization of Eq. (2) to obtain $\hat{\phi}_{n+1}$, and then to solve the control problem which here comes down to finding the DM deterministic best least-square fit to the phase estimate, hence minimizing:

$$\epsilon_{\text{cont}} = \left\| \hat{\phi}_{n+1} - \mathbf{N}\mathbf{u}_n \right\|^2 \tag{7}$$

We consider here a DM with an instantaneous response, but the formalism could be easily extended to account for DM dynamics [5]. Note that the separation principle still holds in this case.

The different sub-problems are now well defined. The solution to these sub-problems are derived and discussed in the following paragraphs.

2.2. WFS reconstruction

We discuss here the question of phase reconstruction from delayed noisy open-loop WFS measurements. As stated in Section 2.1 the optimal reconstruction $\hat{\phi}_{n+1}$ is defined as minimizing Eq. (2).

The estimate $\hat{\phi}_{n+1}$ has to be deduced from the past available WFS data $\{\mathbf{s}_n, \mathbf{s}_{n-1}, \mathbf{s}_{n-2}, \ldots\}$. We therefore have to perform an optimal inversion of the measurement equation using both the spatial and temporal priors (cf. Eqs. (3) and (4)) to regularize the process and extract as best as we can the signal from the noisy data. Since we look for an estimate of ϕ_{n+1} from data related, at the latest, to ϕ_{n-dr} the estimation also implicitly includes a temporal extrapolation, namely a prediction at $dr+1$ time steps.

With the linear models described in Section 2.1 and Gaussian priors, the optimal estimate $\hat{\phi}_{n+1}$ is the conditional expectation of ϕ_{n+1} with respect to the measurement data $\{\mathbf{s}_n, \mathbf{s}_{n-1}, \mathbf{s}_{n-2}, \ldots\}$, which can be computed iteratively as the output of a Kalman filter [21]. The matrices involved in this computation are deduced from the matrices characterizing the system and the turbulence.

For illustration we give here the optimal solution in the case of a one frame read-out delay ($dr = 1$), hence a two frame total delay. The standard formulation consists in rewriting the measurement and evolution equations (see Eqs. (1) and (3)) in a state space representation. The two frame delay implies that the state vector $\mathbf{X}_n$ includes the phase at three time steps, that is $\mathbf{X}_n^t = (\phi_{n+1}, \phi_n, \phi_{n-1})$. The state model composed of respectively the evolution and measurement equations then reads:

$$\mathbf{X}_{n+1} = \begin{pmatrix} \mathbf{A}_{\text{tur}} & 0 & 0 \\ \mathbf{Id} & 0 & 0 \\ 0 & \mathbf{Id} & 0 \end{pmatrix} \mathbf{X}_n + \begin{pmatrix} \mathbf{Id} \\ 0 \\ 0 \end{pmatrix} \nu_n \tag{8}$$

$$\mathbf{Y}_n = \mathbf{D}\begin{pmatrix} 0 & 0 & \mathbf{Id} \end{pmatrix} \mathbf{X}_n + \mathbf{w}_n \tag{9}$$

where $\mathbf{Y}_n$ corresponds here to the WFS measurement $\mathbf{s}_n$. Hence the standard compact form:

$$\mathbf{X}_{n+1} = \mathscr{A}\mathbf{X}_n + \mathbf{V}_n \tag{10}$$

$$\mathbf{Y}_n = \mathscr{C}\mathbf{X}_n + \mathbf{w}_n \tag{11}$$

Standard linear optimal filtering theory then gives the optimal estimation in the following form:

$$\hat{\mathbf{X}}_{n+1/n} = \mathscr{A}\hat{\mathbf{X}}_{n/n-1} + \mathscr{A}\mathbf{H}_n\left(\mathbf{y}_n - \mathscr{C}\hat{\mathbf{X}}_{n/n-1}\right) = \mathscr{A}\hat{\mathbf{X}}_{n/n-1} + \mathscr{A}\mathbf{H}_n\left(\mathbf{s}_n - \mathbf{D}\hat{\phi}_{n-1/n-1}\right) \tag{12}$$

$\hat{\mathbf{X}}_{n+1/n}$ is the optimal estimation of $\mathbf{X}_{n+1}$ using the measurements acquired till time step n and the priors. Similarly $\hat{\phi}_{n-1/n-1}$ is the estimate of the phase at time $n-1$ using measurements acquired till step $n-1$. The second component of $\hat{\mathbf{X}}_{n+1/n}$ gives the requested phase estimate $\hat{\phi}_{n+1}$. The difference between the last available data $\mathbf{y}_n = \mathbf{s}_n$ and its estimated counter-part $\mathbf{D}\hat{\phi}_{n-1/n-1}$ is called innovation. A recursive up-date equation such as Eq. (12) is called an observer: one step of prediction according to the evolution equation applied to the sum of the previous state prediction and of an observer gain applied to the innovation.

The optimal observer gain $\mathbf{H}_n$ provides a trade-off between model-based prediction and measurements, it is given by:

$$\mathbf{H}_n = \mathbf{C}_{n/n-1}\mathscr{C}^t\left(\mathscr{C}\mathbf{C}_{n/n-1}\mathscr{C}^t + \mathbf{C}_w\right)^{-1} \tag{13}$$

where $\mathbf{C}_{n/n-1}$ is the covariance matrix of the state estimation error. $\mathbf{C}_{n/n-1}$ is computed by solving the Ricatti equation [22]:

$$\mathbf{C}_{n+1/n} = \mathscr{A}\mathbf{C}_{n/n-1}\mathscr{A}^t + \mathbf{C}_v - \mathscr{A}\mathbf{C}_{n/n-1}\mathscr{C}^t\left(\mathscr{C}\mathbf{C}_{n/n-1}\mathscr{C}^t + \mathbf{C}_w\right)^{-1}\mathscr{C}\mathbf{C}_{n/n-1}\mathscr{A}^t \tag{14}$$

As this equation is independent from the data acquired during the closed-loop, it can be computed off-line. Since the observer gain is shown to have a fast convergence one can actually replace $\mathbf{H}_n$ in Eq. (12) by a constant matrix $\mathbf{H}_\infty$ corresponding to its asymptotic value [6].

It is important to note that the optimal estimation up-date equation (Eq. (12)) and its observer gain (Eq. (13)) directly derive from the physical priors on the turbulence and on the system.

In the unrealistic case of no delay (formally $dr = -1$), no prediction is implied and the optimal solution comes down to the standard recursive least square solution. Another degenerated case is the one shot optimal reconstruction of a turbulent phase from a single WFS measurement of this phase. The optimal solution is in this case the standard regularized inversion of

Eq. (1) [7]. When dealing with time series, one could think of applying this one shot regularized inverse to the last WFS data. Of course this is far from optimal. In particular such a solution would not benefit from a temporal filtering of the noise while the recursive Kalman estimation does, thanks to the temporal priors.

An even cruder approach would consist in performing a least-square best fit to the last available WFS data, that is looking for $\hat{\phi}^{ls}_{n+1}$ that minimizes $\|\mathbf{s}_n - \mathbf{D}\hat{\phi}_{n+1}\|^2$. Note that this deterministic criterion provides a best fit to the data, which is not very relevant for high resolution imaging. It leads to the generalized inverse solution: $\hat{\phi}^{ls}_{n+1} = (\mathbf{D}^t\mathbf{D})^{-1}\mathbf{D}^t\mathbf{s}_n = \mathbf{R}_{ls}\mathbf{s}_n$. However, $\mathbf{D}^t\mathbf{D}$ is generally badly conditioned, a truncation of the Zernike basis, or a truncated SVD is required which leads to a poorly controlled solution with an implicit ad-hoc regularization. The available priors on the turbulence are not explicitly used, there is no attempt of performing a temporal prediction, and it is a one shot estimation with no temporal filtering of the noise.

2.3. Open-loop correction

In the open-loop configuration the correction is provided by a DM which is not seen by the WFS channel. Such an approach is not used in current AO systems since it would require a high dynamic WFS and since open-loop performance could be rather sensitive to calibration errors. It is still an option under investigation for the future Multi-Object AO (MOAO) projects [23,24]. In any case, open-loop correction is of formal interest since it is an interesting step before addressing the closed-loop case.

As stated in Section 2.1 the optimization problem consists here in finding the correction voltages that ensure a minimum residual phase variance, that is minimizing Eq. (6). It was said to be equivalent to first solve the optimal reconstruction from open loop data described in Section 2.2, so as to obtain $\hat{\phi}_{n+1}$. The optimal control voltages are then obtained by minimizing the deterministic criterion given in Eq. (7). The minimization of Eq. (7) easily gives the optimal voltages in the form:

$$\mathbf{u}_n = (\mathbf{N}^t\mathbf{N})^{-}\mathbf{N}^t\hat{\phi}_{n+1} = \mathbf{P}\hat{\phi}_{n+1} \tag{15}$$

To summarize, the optimal open-loop correction is solved by a Kalman filter reconstruction of the turbulent phase from open-loop data followed by a projection onto the DM space.

A more naive approach could be to perform a least square fit of the last available data by the DM, that is looking for $\hat{\mathbf{u}}^{ls}_n$ that minimizes $\|\mathbf{s}_n - \mathbf{D}\mathbf{N}\mathbf{u}_n\|^2$. This leads to performing a generalized inverse of the interaction matrix $\mathbf{D}_{\text{inter}} = \mathbf{D}\mathbf{N}$ in the form:

$$\mathbf{u}^{ls}_n = \left(\mathbf{D}^t_{\text{inter}}\mathbf{D}_{\text{inter}}\right)^{-}\mathbf{D}^t_{\text{inter}}\mathbf{s}_n = \mathbf{R}_{\text{com}}\mathbf{s}_n \tag{16}$$

This is similar to the least-square wave-front reconstruction mentioned at the end of Section 2.2 and the same limitations apply here (no prediction, no temporal filtering, ...). The restriction to the DM space brings here the implicit regularization that stabilizes the solution, but the condition number is still often very large due to unseen, alias waffle, modes and additional tricks are generally required to filter out such components. The fact that this approach does not distinguish the phase estimation part from the mirror control aspects is indeed limiting. The explicit phase estimation, using physical priors, performed in the optimal estimation should allow a better treatment of aliasing and waffle effects. The importance of an explicit estimation of the turbulent phase in MCAO will also be emphasized in Section 2.5.

2.4. Closed-loop correction

In the closed-loop mode, the WFS sees residual phases corrected by the DM. The measurement equation is then modified accordingly (see Section 2.1). Assuming that the contribution of the DM to the closed loop measurement ($\mathbf{s}^{\text{closed}}_n$) is perfectly known ($\mathbf{D}\mathbf{N}\mathbf{u}_{n-dr-1}$), the problem is formally equivalent to the open-loop case. The separation principle still applies and the optimal phase estimate is obtained with the same Kalman filter equations (see Section 2.2), one has only to replace in the observer equation the open-loop WFS measurement by the synthesized open-loop one. In Eq. (12), corresponding to a two frame delay, it means to replace $\mathbf{s}_n$ by $\mathbf{s}^{\text{closed}}_n - \mathbf{D}\mathbf{N}\mathbf{u}_{n-2}$. The optimal voltages are still given by Eq. (15).

It is therefore interesting to note that, provided the model is correct, we have two equivalent systems, respectively open and closed-loop, with a simple transposition between the open and closed-loop control law. However, one has to keep in mind that the robustness in stability and performance will be different in the closed-loop and open-loop cases. A specific study has to be performed particularly to estimate the impact of uncertainties on the WFS and DM model.

We now recall for comparison the conventional approach used in current AO systems [25]. It is based on an integrator control law, the voltage increments being computed from the closed-loop WFS data by least-square reconstruction. This can be summarized by the following equations:

$$\delta\mathbf{u}^{ls}_n = \left(\mathbf{D}^t_{\text{inter}}\mathbf{D}_{\text{inter}}\right)^{-}\mathbf{D}^t_{\text{inter}}\mathbf{s}_n = \mathbf{R}_{\text{com}}\mathbf{s}_n \tag{17}$$

$$\mathbf{u}_n = \mathbf{u}_{n-1} + g\,\delta\mathbf{u}^{ls}_n \tag{18}$$

where g is the integrator gain represented here as a global scalar gain. The gain can also be optimized mode per mode accounting for priors on modal temporal behavior and noise level, this is the so-called Optimized Modal Gain Integrator [OMGI] [10,11]. Even if the OMGI procedure has been applied successfully on current AO systems, one can list several drawbacks that might limit its application in future developments (XAO [26], MCAO, ...). The optimization is not global: the multi-variable servo-loop is split in individual scalar, supposedly independent, loops. Unseen modes are still brutally filtered out. In this framework the choice of the modes has an influence, and is often difficult to justify. The choice of the control law itself, here an integrator, is ad-hoc and does not derive from the physical priors. One can actually rewrite the integrator control in an observer form [27] to show that it supposes implicitly an underlying evolution equation for the turbulent phase. This implicit model is not physically sound since it can be shown to have an unbounded energy. This is at the origin of the notorious wind-up effect for controllers with integral action. Similarly, any linear AO control, such as predictive controllers [12], can be traced back to an observer, and thus leads to an implicit turbulent phase model [27]. Besides, if the observer gain does not match the Kalman one, the control is sub-optimal with respect to the minimum variance criterion.

Contrary to the mode per mode approaches, our optimal resolution of the multi-variable servo-loop leads to a control law derived in a natural manner from the physical inputs on the system and perturbations to be corrected. For instance if the perturbation to be corrected exhibits vibrations in addition to the turbulence, one can take them into account by modifying the state equations accordingly. A new optimal control law can then be derived and is shown to provide both a good correction of turbulence and a huge damping of vibrations [8]. This asset is all the more relevant for XAO.

Note also that if the computation cost of optimal control is a few times higher than with standard techniques, it still remains of the same order. We remind that the resolution of Ricatti equation (Eq. (14)) is performed off-line before launching the Real Time Computer (RTC). Besides the increase with telescope diameter of the computation cost follows the usual scaling laws.

2.5. Specificities of MCAO

The equations presented in the previous sections are rather general, and they can easily be extended to the MCAO case. Up to now the turbulent estimates and correction phases were in the instrument pupil. In MCAO [28] one has to account for the distribution of turbulence in the volume, which leads to a FoV dependent perturbation, and for possibly several DMs which leads to a FoV dependent correction. Generally, several WFSs pointing at several Guide Stars (GSs) are also used to probe the turbulence volume.

The volumic turbulent phase is generally modeled by phases in L layers, represented by a meta-vector $\varphi = \{\varphi_k\}$, each φ_k being a vector of Zernike coefficients describing the phase in altitude on given meta-pupils. Neglecting diffraction effects, the resulting phase in a given direction α is derived from the volumic phase by a linear relation: $\phi(\alpha) = M_\alpha^L \varphi$. A measurement equation can then be deduced for each of the N_{gs} GSs. Piling-up the individual measurements $\mathbf{s}_i$ one obtains a unique measurement equation quite similar to Eq. (1) with generalized vectors and matrices.

Concerning turbulence priors, one assumes independent layers leading to a block diagonal covariance matrix C_φ for the volumic phase. Each block is deduced from Noll with a scaling that accounts for turbulence strength distribution in altitude. Similarly a generalized block diagonal matrix $\mathbf{A}_{\text{tur}}$ is used to describe temporal effects, and accounts then for the wind speed profile.

The optimal wave-front reconstruction in the volume $\hat{\varphi}_n$ minimizes the criterion $\langle \|\varphi_{n+1} - \hat{\varphi}_{n+1}\|^2 \rangle_{\text{turb,noise}}$. The solution is given by the Kalman filter, which leads to equations similar to Eqs. (8)–(14) applied to generalized vectors/matrices [6]. This reconstruction of the turbulent volume from WFS measurements of its projection in particular directions is often called 'tomographic reconstruction'.

Concerning the optimal correction issue, one has first to define the optimality criterion. We still seek the DM voltages minimizing the residual phase variance, but one has to specify in which Scientific FoV of interest (SFoV). The criterion then reads:

$$\left\langle \int_{\text{SFoV}} \left\| \phi_{n+1}(\alpha) - \phi_{n+1}^{\text{cor}}(\alpha) \right\|^2 \mathrm{d}\alpha \right\rangle_{\text{turb,noise}} = \left\langle \int_{\text{SFoV}} \left\| M_\alpha^L \varphi_{n+1} - M_\alpha^{\text{DM}} \mathbf{N} \mathbf{u}_n \right\|^2 \mathrm{d}\alpha \right\rangle_{\text{turb,noise}}$$

where $\mathbf{N}$ is a generalized influence matrix characterizing the different DMs, M_α^{DM} gives the correction in the position α in the FoV.

As the separation principle still applies, the optimal voltages $\mathbf{u}_n$ are thus obtained by projection of the Kalman estimate $\hat{\varphi}_{n+1}$ onto the DMs so as to minimize the deterministic criterion: $\int_{\text{SFoV}} \| M_\alpha^L \hat{\varphi}_{n+1} - M_\alpha^{\text{DM}} \mathbf{N} \mathbf{u}_n \|^2 \, \mathrm{d}\alpha$. The projection matrix is easily derived [6] and accounts for the Scientific FoV, for the DM influence functions and altitude of conjugation. The solution takes the form: $\mathbf{u}_n = \mathbf{P}(\text{SFoV}, \{h_j^{\text{DM}}\}) \hat{\varphi}_{n+1}$. Note that all the equations developed before can be generalized to weighted averages in the SFoV.

Of course, one can think of generalizing classic AO control to MCAO. However, the drawbacks mentioned before are more penalizing in this context: a least-square fit by the DMs of the WFS data will optimize the correction in the GS directions,

leading to a poor control of the correction in the rest of the FoV. The SFoV cannot be specified in standard approaches. This is related to the handling of unseen modes. In MCAO estimating these modes (that have no impact in the GS directions) means performing a good interpolation of the perturbation between GS and in turns a good correction in these regions. Standard methods simply filter out these components, whereas global reconstruction permits a global multi-variable treatment which includes an explicit estimation of the turbulent phase thanks to physical priors.

The potential gain in performance brought by optimal control in MCAO has been recently illustrated in simulation [6] for a given representative MCAO system (2 DM and 3 GS configuration). Similarly for given performance specifications optimal control may reduce the system complexity (less or fainter GSs, ...). Besides the implementation in MCAO of the standard OMGI has been shown to be non-trivial due to aliasing effects specific to MCAO configurations [9].

Note that if the SFoV is reduced to a single direction α_o, or a small region around it compared to the isoplanatic patch, then a single DM in the pupil is sufficient since the correction does not have to evolve in the SFoV. When a single GS is available, at a given angle away from the SFoV, this corresponds to the OAAO scheme described in detail in Section 3. In this case, it is, of course, mandatory to dissociate the phase space in the volume and its estimation, from the mirror space in the pupil and its control. The correction phase is a least square fit of the projection along α_o of the optimal volumic phase. An experimental demonstration of the closed-loop real time correction in OAAO is given in Section 3.

If the SFoV is constituted of several well separated regions, each region being smaller than the isoplanatic patch, then one specific DM per sub-field is required. This corresponds to the concept of Multiple Object Adaptive Optics (MOAO) [24], each channel being similar to OAAO except that several GS are generally available for WFS. Besides, for extragalactic MOAO, such as the Falcon project [29], the GSs are faint and far apart. All these elements make Kalman control especially attractive for this application.

Note that prior knowledge on turbulence is required in optimal control. However, it has been shown that performance are not very sensitive to uncertainties on turbulence profile [30,16] and on temporal priors [6]. A careful analysis of the robustness of optimal control is currently under study. One can of course try to estimate the turbulence characteristics from the AO data, and then modify the control law parameters in real time, so-called adaptive control [31]. Nevertheless stability is generally not ensured in such approaches.

3. Tomographic off-axis AO: a first experimental validation

3.1. Principle and experimental set-up

OAAO is a particular case of MCAO with a single GS for WFS and a SFoV reduced to a single direction α_o. A unique DM conjugated to the entrance pupil (diameter D) is then necessary. This is an intermediate concept between MCAO and classic AO. It will allow us, with a simple experiment, to have a first laboratory demonstration of closed-loop optimal control based on a minimum variance tomographic reconstruction (see Sections 2.4 and 2.5). The principle is described in Fig. 2.

We consider a single turbulent layer at altitude h and two stars with an angular separation α_o. The on-axis GS is used to analyze the on-axis turbulence. From these measurements, the turbulence in altitude is estimated, and the deduced off-axis wavefront is corrected by the DM.

OAAO tests have been performed thanks to the classic AO test bench BOA developed by ONERA. It is composed of a turbulence generator, a telescope simulator, the AO system and an imaging camera. The source is a fibered LASER diode working at $\lambda = 633$ nm placed on-axis. The turbulence generator is composed of a phase screen mirror on a rotating stage so as to reproduce the wind effects and placed in the collimated beam. The phase screen mirror is developed by Observatoire de Paris-Meudon and reproduces Kolmogorov turbulence. The turbulence strength corresponds to a $D/r_0 \simeq 2.8$ at 633 nm. Transposed to an 8 m telescope observing at 2.2 μm, this would correspond to a 0.21 arcsec seeing at 500 nm. It is weak but could be representative of the turbulence in altitude.

The wavefront corrector is based on a Tip Tilt Mirror (TTM) and a 9×9 actuator DM. 69 of its actuators are used. The Shack–Hartmann WFS is composed of a 8×8 lenslet array (52 sub-pupils used) and a 128×128 pixel DALSA camera (read out noise of $85e^-$/pixel/frame). The imaging camera is a 512×512 pixel Princeton camera (read out noise $4e^-$/pixel/frame). Note that this AO configuration is designed to work in closed loop, meaning that DM and TTM are placed before the WFS in the optical path.

For OAAO tests, a second source, identical to the first one, has been inserted. The two sources have a fixed angular separation $\alpha_o \simeq 50(\lambda/D)$ so that both sources can be imaged on the Princeton camera. A large pinhole is also placed in the entrance focal plan of the WFS so as to select the on-axis source and stop the light coming from the off-axis one. The AO bench has been calibrated and optimized so that the Strehl Ratio [SR] without turbulence (internal SR) is 84% for the off-axis star [32].

To increase anisoplanatism effects, the turbulent mirror can be translated in altitude. Scintillation effects have been shown to be negligible. Thus, the light beams from both sources intersect the turbulent layer defining two footprints, which are the

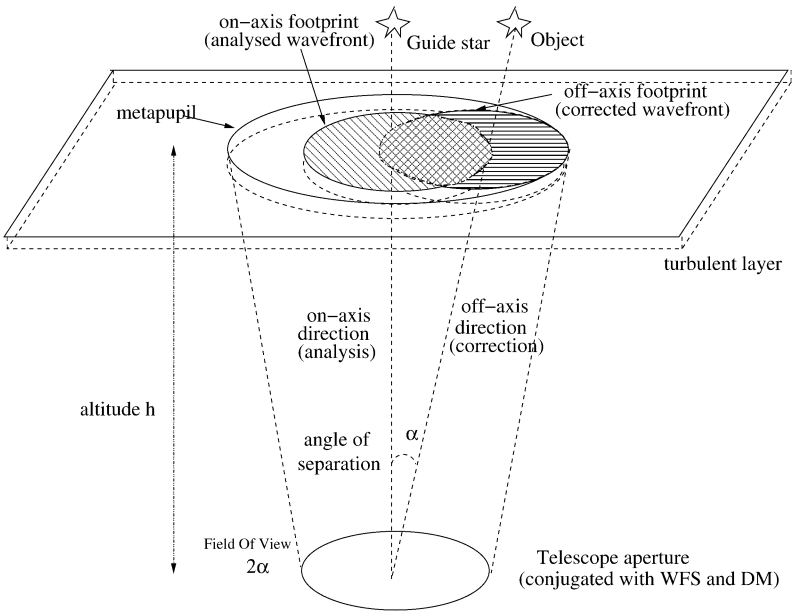

Fig. 2. Principle of OAAO: we consider a single turbulent layer at altitude h and two stars with angular separation α. The projections in the turbulent layer of the entrance pupil in each direction define an on-axis (diagonal pattern) and an off-axis (horizontal pattern) footprint. The footprints relative separation is noted $\delta = \alpha h/D$. The 2α FoV defines a metapupil encircling both footprints. OAAO consists in analyzing the on-axis turbulence to estimate the off-axis turbulent wavefront and correct it with a single DM conjugated with the aperture.

projections of the system aperture. The footprint relative separation δ is related to the altitude h, the angular separation α_o and the pupil diameter D by: $\delta = \alpha_o h/D$. Then by analogy, when the footprint relative separation δ increases from 0 to 40% on the set-up, it is equivalent to an angular separation between two stars ranking from 0 to 4 arcmin for an 8 meter telescope and a 3000 meter high turbulent layer. When $\delta = 0$, the turbulent layer is in the entrance pupil and there is no anisoplanatism. The off-axis star sees the same turbulence as the on-axis one.

A specific RTC has been built by Shaktiware Inc. for our application on a commercial Linux 1.8 GHz PC. Its design gives a very good flexibility for the implementation of various control laws, and in particular for the Kalman based optimal control. According to benchmark tests, this new RTC should perform Kalman based correction up to a 500 Hz sampling rate for 90 estimated modes, or a 130 Hz sampling rate for 300 estimated modes.

The experimental results presented here are obtained with the RTC running at a 60 Hz sampling frequency and with a wind speed V so that $V/D \simeq 0.3$. Note that the wind is in the direction defined by the two stars, the off-axis one being downstream.

3.2. Optimal control results

So as to validate the experimental results, a numerical simulation of the expectable performance of the Kalman filter based closed loop OAAO has been performed. Performance have been simulated thanks to an end-to-end numerical simulator of the experimental set-up. We will first present this simulator and its results before presenting the experimental performance. This simulator reproduces each part of the system, meaning propagation through a Kolmogorov turbulent layer with the corresponding turbulence strength, the WFS analysis with a geometrical model fitted to the OAAO experiment thanks to calibration, and the DM correction with an influence matrix obtained experimentally during a previous calibration campaign. Thus, the numerical simulation particularly matches the experiment. The performance obtained on the simulator also account for the static aberration of the experiment that cannot be corrected for, so that the maximum numerical SR is the internal SR of the bench, that is 84%. Finally, either a classic integrator based or a Kalman filter based control law is applied in the numerical simulator. For both the numerical and experimental simulation, the performance are measured for different footprint relative separations. In each case, the optimal control is adapted to the new footprint relative separation so as to optimize the correction in the off-axis direction taking into account the closed loop on-axis wavefront measurement. The control law and associated matrices correspond to the equations given in Section 2 applied to the particular case of OAAO (single layer, a SFoV corresponding to the off-axis star, ...). The turbulent phase is estimated over 150 Zernike modes.

Fig. 3 shows the evolution of the off-axis performance of the Kalman based optimal control versus a classic AO loop with an integrator, both for the numerical and experimental simulation. In the particular case of integrator based classic AO correction,

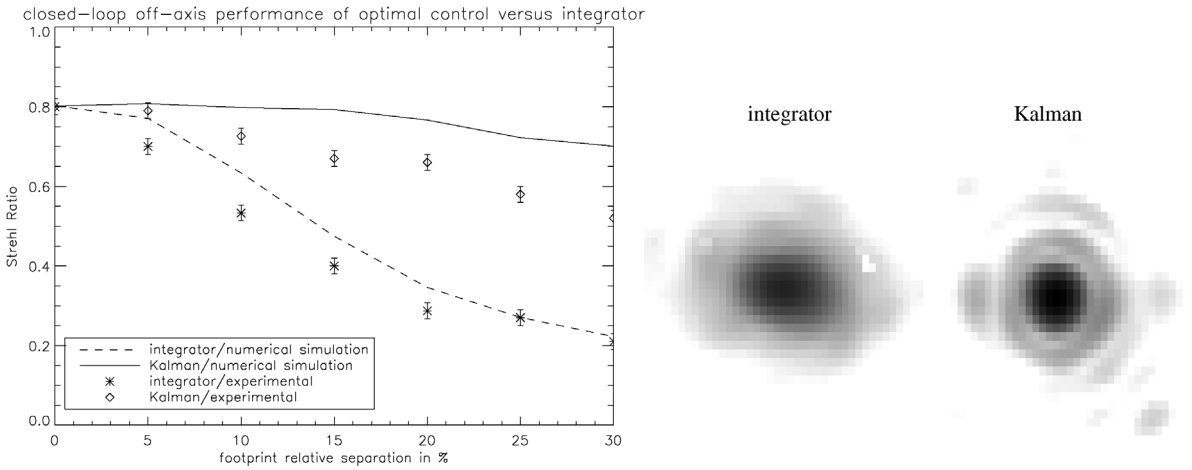

Fig. 3. Right: end-to-end numerical simulation and experimental results of the performance of a Kalman based optimal control in the closed-loop OAAO set-up configuration compared to a classic integrator based AO. The Strehl Ratio is given for the off-axis star according to the footprint relative separation in %. The solid line is the numerical Kalman based control performance, the dashed line is obtained with a classic integrator. Experimental points are also plotted: diamonds are Kalman based optimal control, stars are classic integrator based control. Left: off-axis PSF obtained for a 20% relative separation, either with integrator (left) or Kalman filter (right).

the gain has been optimized on-axis (or equivalently when $\delta = 0$), so that the on-axis performance is the highest for this kind of control law that is a 80% SR. First, considering the numerical simulation results (solid line for Kalman and dashed line for integrator), we can see that a huge improvement of the off-axis SR is expected even for high footprint relative separations. The Kalman off-axis SR is nearly constant at 80% up to $\delta = 20\%$, while with a classic integrator controller, the off-axis SR decreases steadily due to anisoplanatism effects.

Now, first results have been obtained with the experiment and are also presented on Fig. 3. Comparing numerical and experimental performances, a good agreement is obtained. The overall behaviors are similar to the expected ones for both controller. A large improvement of the off-axis SR is indeed obtained with the Kalman based optimal control. For instance, when $\delta = 20\%$ (2 arcmin angular separation between the stars according to our analogy for a 8 m telescope see Section 3.1), the experimental integrator SR is about 27% while the Kalman one is as high as 66%. Experimental PSFs, obtained with Kalman based optimal control or classic integrator based AO, are also given in Fig. 3 in this particular case of a 20% footprint relative separation.

Nevertheless, some differences appear between numerical and experimental results for both controllers. The integrator SR decreases slightly faster in the experimental case. The Kalman performance is lower than in the numerical simulation. These differences can be due first to errors in the model of the simulator as of course the numerical description does not encompass all the details or defects of the set-up (in particular the phase screen mirror does not have perfect Kolmogorov statistics). However, in the particular case of the Kalman based optimal control, model approximations when defining the Kalman matrices can also explain the loss of performance. This point is currently under study.

Still, this is the first demonstration of closed-loop off-axis optimal correction. It demonstrates the impressive improvement of the correction in a large field of view brought by optimal control. One could object that considering a unique layer is a favorable case. However one has to keep in mind that only one GS is available for WFS, hence very limited measurements.

Theses results prove the high potential of Kalman based optimal control for MCAO and MOAO compared to classic approaches.

4. Conclusions

We have presented an optimal approach for open/closed loop correction in AO and MCAO. It is based on an optimal reconstruction of the phase from WFS data. This estimation takes the form of a Kalman filter. It accounts for the loop temporal delays and uses the available temporal and spatial priors (temporal correlation, turbulence statistics and profile). The correction commands are then deduced from the estimated phase by a projection onto the DM space.

With optimal control only a slight improvement is expected for the correction of turbulence in classic AO, compared to more standard controllers. However, its flexibility allows us to easily account for parasitic perturbations. For instance, this control law

provides, in addition to a good correction of turbulence, a huge damping of vibrations thanks to temporal prediction [8]. This asset is all the more relevant for XAO.

The approach is of course particularly suited for MCAO: the estimation step provides an optimal tomographic reconstruction, hence an efficient interpolation of the wave-front between the different GSs, while the correction can be specified for a given FoV of interest [6]. It applies to different WFS strategies [33] (Layer [34] or Star Oriented), with both Laser GSs (LGSs) [35] and Natural GS. Numerical simulations are very encouraging. An experimental demonstration is now needed. The implementation of our control law on the MAD MCAO system currently developed at ESO [36] is planned. As a first step a laboratory demonstration of the concept is presented here in the particular case of OAAO. While a classic AO controller barely reaches a 27% SR for a 20% footprint relative separation (2 arcmin equivalent angular separation), our Kalman based approach achieves a 66% SR. This highly significant improvement is also in good agreement with numerical simulations.

MOAO is very similar to OAAO except that it uses several faint and far apart GSs. This makes Kalman control especially attractive for this application. The interest of our control approach for Ground Layer AO (GLAO) [37] could also be investigated. The specification of the FoV of interest could be helpful to improve the correction uniformity.

More generally, optimal control should be very useful in demanding conditions: restricting WFS geometries (faint and/or limited number of GSs, LGS) requiring a careful tomographic reconstruction, and specific correction cases (limited number of DMs, particular SFoV, ...). Reciprocally for a given performance specification optimal control can allow to reduce the system complexity (less or fainter GSs, ...).

Acknowledgements

Part of this study has been supported by EC contract RII3-CT-2004-001566. The authors thank B. Le Roux, L. Mugnier and F. Quirós-Pacheco with whom this work has been initiated. We are grateful to F. Mendez and B. Fleury for their help on the experiment, and to F. Chemla, P. Jagourel and F. Hammer for their support.

References

[1] F. Roddier (Ed.), Adaptive Optics in Astronomy, Cambridge University Press, Cambridge, 1999.
[2] R.H. Dicke, Phase-contrast detection of telescope seeing and their correction, Astron. J. 198 (4) (1975) 605–615.
[3] J.M. Beckers, Increasing the size of the isoplanatic patch with multiconjugate adaptive optics, in: M.-H. Ulrich (Ed.), Very Large Telescopes and their Instrumentation, in: ESO Conference and Workshop Proceedings, vol. 2, ESO, Garching, Germany, 1988, pp. 693–703.
[4] D.C. Johnston, B.M. Welsh, Analysis of multiconjugate adaptive optics, J. Opt. Soc. Am. A 11 (1994) 394–408.
[5] R. Paschall, D. Anderson, Linear quadratic Gaussian control of a deformable mirror adaptive optics system with time-delayed measurements, Appl. Opt. 32 (31) (1993) 6347–6358.
[6] B. Le Roux, J.-M. Conan, C. Kulcsár, H.-F. Raynaud, L.M. Mugnier, T. Fusco, Optimal control law for classical and multiconjugate adaptive optics, J. Opt. Soc. Am. A 21 (2004).
[7] T. Fusco, J.-M. Conan, G. Rousset, L.M. Mugnier, V. Michau, Optimal wavefront reconstruction strategies for multiconjugate adaptive optics, J. Opt. Soc. Am. A 18 (2001) 2527–2538.
[8] C. Petit, F. Quirós-Pacheco, J.-M. Conan, C. Kulcsár, H.-F. Raynaud, T. Fusco, G. Rousset, Kalman filter based control loop for adaptive optics, in: Advancements in Adaptive Optics, in: Proc. Soc. Photo-Opt. Instrum. Eng., vol. 5490, SPIE, 2004 (Date conference: June 2004, Glasgow, UK).
[9] F. Quirós-Pacheco, C. Petit, J.-M. Conan, T. Fusco, E. Marchetti, Control law for the multiconjugate adaptive optics demonstrator (MAD), in: Advancements in Adaptive Optics, in: Proc. Soc. Photo-Opt. Instrum. Eng., vol. 5490, 2004 (Date conference: June 2004, Glasgow, UK).
[10] E. Gendron, P. Léna, Astronomical adaptive optics. I. Modal control optimization, Astron. Astrophys. 291 (1994) 337–347.
[11] E. Gendron, P. Léna, Astronomical adaptive optics. II. Experimental results of an optimize modal control, Astron. Astrophys. 111 (1994) 153–167.
[12] C. Dessenne, P.-Y. Madec, G. Rousset, Optimization of a predictive controller for closed-loop adaptive optics, Appl. Opt. 37 (July 1998) 4623–4633.
[13] B. Ellerbroek, T. Rhoadarmer, Adaptive wave-front algorithms for closed loop adaptive optics, Math. Comput. Modelling 33 (2001) 145–158.
[14] C. Petit, J.-M. Conan, C. Kulcsár, H.-F. Raynaud, T. Fusco, J. Montri, Off-axis adaptive optics with optimal control: Laboratory validation, vol. AWA 4, Optical Society of America (OSA), 2005 (Date conference: June 2005, Charlotte, USA).
[15] C. Petit, J.-M. Conan, C. Kulcsár, H.-F. Raynaud, T. Fusco, J. Montri, F. Chemla, D. Rabaud, Off-axis adaptive optics with optimal control: Experimental and numerical validation, in: Advancements in Adaptive Optics, in: Proc. Soc. Photo-Opt. Instrum. Eng., vol. 5903, SPIE, 2005 (Date conference: June 2005, San Diego, USA).
[16] B. Le Roux, Commande optimale en optique adaptative classique et multiconjuguée, PhD thesis, Université de Nice Sophia-Antipolis, 2003.

[17] R.J. Noll, Zernike polynomials and atmospheric turbulence, J. Opt. Soc. Am. 66 (3) (1976) 207–211.
[18] B. Le Roux, J.-M. Conan, C. Kulcsár, H.-F. Raynaud, L.M. Mugnier, T. Fusco, Optimal control law for multiconjugate adaptive optics, in: P.L. Wizinowich, D. Bonaccini (Eds.), Adaptive Optical System Technology II, in: Proc. Soc. Photo-Opt. Instrum. Eng., vol. 4839, SPIE, Hawaii, USA, 2002.
[19] D. Gavel, D. Wiberg, Toward Strehl-optimizing adaptive optics controllers, in: P.L. Wizinowich (Ed.), Adaptive Optical Systems Technologies II, in: Proc. SPIE, vol. 4839-107, 2002.
[20] P. Joseph, J. Tou, On linear control theory, AIEE Trans. Appl. Indus. (1961) 193–196.
[21] B.D.O. Anderson, J.B. Moore, Optimal Control, Linear Quadratic Methods, Prentice-Hall, London, 1990.
[22] H. Van Trees, Detection, Estimation and Modulation Theory, Part I, Wiley, New York, 1968.
[23] F. Assémat, F. Hammer, E. Gendron, P. Laporte, M. Marteaud, M. Puech, J.-M. Conan, T. Fusco, A. Liotard, F. Zamkotsian, FALCON: a new-generation spectrograph with adaptive optics for the ESO VLT, in: J.D. Gonglewski, K. Stein (Eds.), Optics in Atmospheric Propagation and Adaptive Systems VI, in: Proc. Soc. Photo-Opt. Instrum. Eng., vol. 5237, 2004.
[24] E. Gendron, F. Assémat, F. Hammer, P. Jagourel, F. Chemla, P. Laporte, M. Puech, M. Marteaud, F. Zamkotsian, A. Liotard, J.-M. Conan, T. Fusco, N. Hubin, FALCON: multi-object AO, C. R. Physique 6 (2005), this issue.
[25] P.-Y. Madec, Control techniques, in: Roddier [1], Ch. 6, pp. 131–154.
[26] T. Fusco, G. Rousset, J.-L. Beuzit, D. Mouillet, K. Dohlen, R. Conan, C. Petit, G. Montagnier, Conceptual design of an extreme AO dedicated to extra-solar planet detection by the VLT-planet finder instrument, in: Astronomical Adaptive Optics Systems and Applications II, in: Proc. Soc. Photo-Opt. Instrum. Eng., vol. 5903, SPIE, 2005 (Date conference: July 2005, San Diego, USA).
[27] C. Kulcsár, H.-F. Raynaud, C. Petit, J.-M. Conan, B. Le Roux, Optimality, observers and correctors in adaptive optics, vol. AWC 1, Optical Society of America (OSA), 2005 (Date conference: June 2005, Charlotte, USA).
[28] S. Esposito, Introduction to multi-conjugate adaptive optics systems, C. R. Physique 6 (2005), this issue.
[29] F. Hammer, F. Sayède, E. Gendron, T. Fusco, Scientific drivers for ESO future VLT/VLTI instrumentation, Proc. SPIE (2001) 139.
[30] J.-M. Conan, B. Le Roux, D. Bello, T. Fusco, G. Rousset, Optimal reconstruction in multiconjugate adaptive optics, in: E. Vernet, R. Ragazzoni, S. Esposito, N. Hubin (Eds.), Beyond Conventional Adaptive Optics, Astronomical Observatory of Padova, ESO, Garching-bei-München, Germany, 2002, pp. 209–216 (Date conference: May 2001).
[31] J.S. Gibson, C.-C. Chang, B.L. Ellerbroek, Adaptive optics: wave-front correction by use of adaptive filtering and control, Appl. Opt. 39 (16) (2000) 2525–2538.
[32] T. Fusco, C. Petit, G. Rousset, J.-F. Sauvage, J.-M. Conan, Optimization of the pre-compensation of non-common path aberrations for adaptive optics systems, vol. AWB 1, Optical Society of America (OSA), 2005 (Date conference: June 2005, Charlotte, USA).
[33] T. Fusco, M. Nicolle, G. Rousset, V. Michau, A. Blanc, J.-L. Beuzit, J.-M. Conan, Wavefront sensing issues in MCAO, C. R. Physique 6 (2005), this issue.
[34] R. Ragazzoni, J. Farinato, E. Marchetti, Adaptive optics for 100 m class telescopes: new challenges require new solutions, Proc. SPIE 4007 (2000) 1076–1087.
[35] F. Rigaut, C. d'Orgeville, On practical aspects of laser guide stars, C. R. Physique 6 (2005), this issue.
[36] E. Marchetti, R. Brast, B. Delabre, R. Donaldson, E. Fedrigo, C. Frank, N. Hubin, J. Kolb, M. Le Louarn, J.-L. Lizon, S. Oberti, F. Quirós-Pacheco, R. Reiss, J. Santos, E. Vernet, S. Tordo, R. Ragazzoni, S. Arcidiacono, P. Bagnara, A. Baruffolo, E. Diolaiti, J. Farinato, M. Lombini, MAD: practical implementation of MCAO concepts, C. R. Physique 6 (2005), this issue.
[37] F. Rigaut, Ground-conjugate wide field adaptive optics for the ELTs, in: E. Vernet, R. Ragazzoni, S. Esposito (Eds.), Beyond Conventional Adaptive Optics, Padova, Italy, Proc. ESO, 2001, p. 58.